

Magnetism in graphene nanoribbons on Ni(111): First-principles density functional study

| | |
|-------|---|
| メタデータ | 言語: eng 出版者: 公開日: 2022-03-10 キーワード (Ja): キーワード (En): 作成者: メールアドレス: 所属: |
| URL | https://doi.org/10.24517/00065553 |

This work is licensed under a Creative Commons Attribution-NonCommercial-ShareAlike 3.0 International License.



Magnetism in graphene nanoribbons on Ni(111): First-principles density functional studyK. Sawada,¹ F. Ishii,¹ and M. Saito^{1,2}¹*Division of Mathematical and Physical Science, Graduate School of Natural Science and Technology, Kanazawa University, Kakuma, Kanazawa 920-1192, Japan*²*Collaborative Research Center for Frontier Simulation Software for Industrial Science, Institute of Industrial Science, University of Tokyo, 4-6-1 Komaba, Meguroku, Tokyo 153-8505, Japan*

(Received 18 August 2010; revised manuscript received 19 November 2010; published 22 December 2010)

We study magnetism of zigzag graphene nanoribbons (ZGNRs) whose ribbon widths are 1.8–2.2 nm by performing first-principles density functional theory calculations. In contrast with freestanding ZGNRs, ZGNRs directly adsorbed on Ni(111) do not show *flat-band magnetism* due to strong orbital hybridization between edge-localized C *p* orbitals and Ni *d* orbitals. The flat-band magnetism of the ZGNR is recovered by introduction of a graphene sheet between the ZGNR and Ni(111) as a buffer layer which weakened the orbital hybridization. In this case, a parallel configuration of spin moments at the two edges has lower energy than the antiparallel spin configuration whereas the magnetic ground state of the freestanding ZGNR has an antiparallel spin configuration. We explore the effects of orbital hybridization and charge transfer on the magnetic stability of ZGNRs on graphene/Ni(111).

DOI: [10.1103/PhysRevB.82.245426](https://doi.org/10.1103/PhysRevB.82.245426)

PACS number(s): 73.22.Pr, 71.15.-m, 75.75.-c, 81.05.ue

I. INTRODUCTION

Graphene, a two-dimensional honeycomb lattice consisting of C atoms, shows useful properties for spintronics applications. The spin transport has been observed in monolayer and multilayer graphenes experimentally.^{1–3} The spin injection was succeeded in room temperature, convincing realization of graphene spintronics devices in future.

Zigzag graphene nanoribbons (ZGNRs) are important in spintronics application because ZGNRs shows *flat-band magnetism* induced by peculiar localized electronic states at each edge.^{4,5} Previous first-principles calculations predicted that the magnetic ground state of the ZGNR is an antiparallel interedge spin (APIES) state: two ferromagnetic (FM) chains at the edges have opposite spin directions.⁶ The cancellation of ferromagnetic spin moment at each edge leads to the *zero* total magnetization of ZGNR. Substantial total magnetization of ZGNR is expected to open a gateway into a spintronics application. So, there were several attempts to obtain finite magnetization in ZGNRs.⁷ It was predicted that the ZGNR is magnetized when the numbers of monohydrogenated and dihydrogenated carbons are different.⁸ It was recently found that the magnetization of ZGNRs can be achieved by carrier doping: As carriers increase the magnetic state is changed from the APIES to the parallel-interedge spin (PIES) state through the noncollinear interedge spin state.⁷

So far, magnetism of freestanding systems of the monolayer type^{4–8} and of multilayer types^{9–11} have been mainly studied. Since nanodevices are structured on substrates in practical applications, understanding of effects of substrates on magnetic properties of ZGNRs is necessary. The structural and electronic properties of graphene on substrates, such as Ni(111),¹² Co(0001),¹³ Ru(0001),¹⁴ Ir(111),¹⁵ SiC,¹⁶ and SiO₂ (Ref. 17) were reported. Among them, the Ni(111) substrate is important because of the lattice commensuration.¹⁸ Since the Ni substrate has a FM property, magnetism of ZGNRs is expected to be affected by the mag-

netic interaction between the substrate and ZGNRs. It is also noticed that there is charge transfer from metal substrate to the graphene.¹⁹ It is expected that the magnetic state is also affected by this charge transfer.

In this study, we perform first-principles density functional calculations of the monolayer ZGNR on Ni(111) [Figs. 1(a) and 1(b)] and the ZGNR on a graphene sheet over Ni(111) [ZGNR/graphene on Ni(111)] [Fig. 1(c)]. We reveal that magnetic moments of edges in the monolayer ZGNR on Ni(111) are very small and do not show flat-band magnetism. On the other hand, we find that the magnetic moments of edges are substantial in the case of the ZGNR/graphene on Ni(111). The magnitude of the moment is comparable with that in the freestanding case. The PIES state is the most stable and the direction of the magnetic moment of the

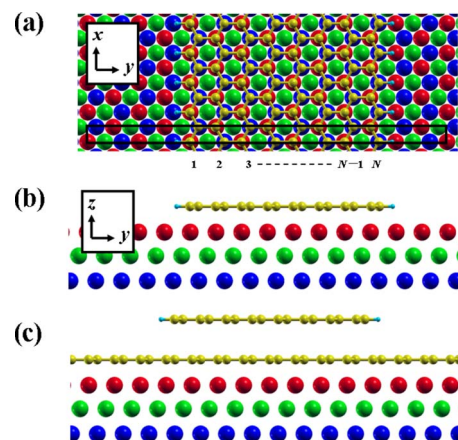


FIG. 1. (Color online) Atomic structure of the ZGNRs ($N=8$) on Ni(111). The yellow (middle size) and light blue (smallest size) spheres denote C and H atoms, respectively. The red, green, and blue (largest size) spheres denote the Ni atom at the first, second, and third layers, respectively. (a) and (b) show the xy plane and yz plane for the monolayer ZGNR on Ni(111). The rectangle in (a) denotes the unit cell and N represents the ribbon width of the ZGNR. (c) shows the yz plane for the ZGNR/graphene on Ni(111).

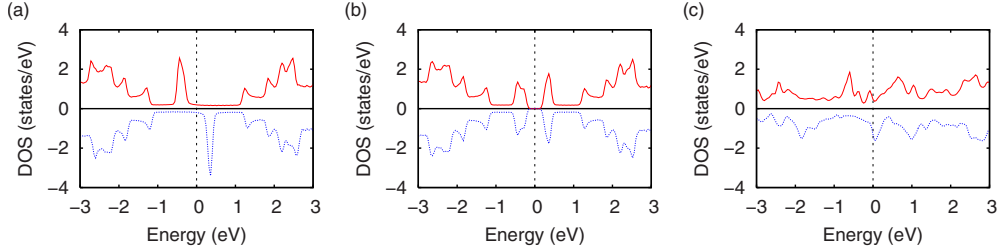


FIG. 2. (Color online) DOS of freestanding ZGNRs having the (a) PIES and (b) APIES states, respectively. The PDOS of the ZGNR on Ni(111) is shown in (c). The energy is measured from the Fermi energy. The solid and dashed lines denote the up-spin and down-spin states, respectively.

ZGNR is parallel to that of the substrate. These findings suggest that substrates have significant effects on magnetism of ZGNRs, and thus are important in device applications in future.

II. COMPUTATIONAL METHODS

By using the OPENMX code,²⁰ we perform first-principles electronic-structure calculations based on the density functional theory (DFT) within the generalized gradient approximation.²¹ The norm-conserving pseudopotential method²² is used. We use the linear combination of multiple pseudoatomic orbitals generated by a confinement scheme.^{23,24} The orbitals are specified by H5.0- s^2p^1 , C5.0- s^2p^2 , and Ni6.0- $s^2p^2d^2$: for an example, in the case of the C atom, C5.0- s^2p^2 means that the cutoff radius is 5.0 bohr in the generation by the confinement scheme,^{23,24} and two primitive orbitals for each of s and p components are used. The partial core correction²⁵ is carried out for C and Ni atoms. The magnetic moment for each atom is estimated by a fuzzy cell partitioning method.²⁶

We use slab models to simulate the two systems in Fig. 1. The ribbon width N of the ZGNR is taken to be 8 [Fig. 1(a)] and the unit cell includes 16 C, 2 H, and 42 Ni atoms. We sample 30 k points in the periodic direction (x direction): the total energy varies within only 0.04 meV/cell when 40 k points are used. The ZGNRs in the ribbon direction (y direction) are separated by 12.1 Å. The number of Ni(111) layers are taken to be three and the length of the vacuum region in the z direction is 10.5 Å. When the number of Ni layers is taken to be 4, the most stable spin configuration does not change. The lattice constant in the x direction is taken to be 2.49 Å which is $1/\sqrt{2}$ of the fcc Ni lattice constant 3.52 Å. The value of the lattice constant 2.49 Å corresponds to the fact that the lattice of the graphene expands by 1.2%. This stretched lattice is found to have a negligible effect on the magnetic state: in the case of the freestanding ZGNR, the stretching varies the difference between the total energies of the APIES and PIES states by only 0.2 meV/cell. We use the interlayer distance determined by the low-energy electron-diffraction experiment:¹⁸ the distances between the ZGNR and first Ni layer, between the first and second Ni layers and between the second and third Ni layers are 2.14 Å, 1.96 Å, and 2.09 Å, respectively. The relative horizontal (x - y) positions of the C honeycomb structure to those of the Ni(111) surface are taken to be the same as those of the experiment.¹⁸

In the case of the ZGNR/graphene on Ni(111), we use the AB -stacking structure for the ZGNR and graphene sheet, and the interlayer distance between the ZGNR and graphene is 3.35 Å, which is taken to be the same as the experimental interlayer distance of graphite.

In Sec. III C, we will study the ZGNR/graphene on Ni. As was mentioned above, we use the experimental values for the positions of the C honeycomb structure of the graphene on the Ni(111) surface. When we optimize the relative horizontal (x - y) positions of the C honeycomb structure to those of the Ni(111) surface, the atomic position is relaxed within 0.05 Å and thus this relaxation effect on the energetics can be neglected. Actually we find that the relative energies among the three magnetic states studied in Sec. III C vary by at most 0.4 meV/cell.

III. RESULTS AND DISCUSSION

A. ZGNR on Ni

We first study the monolayer ZGNR on the Ni(111) substrate. In the cases of freestanding ZGNRs having the APIES and PIES states, the peaks of the density of states (DOS) originating from the edge state appear near the Fermi energies [Figs. 2(a) and 2(b)].^{4,5} On the other hand, these peaks disappear in the case of the ZGNR on Ni(111) [Fig. 2(c)] due to strong orbital hybridization between edge-localized p or-

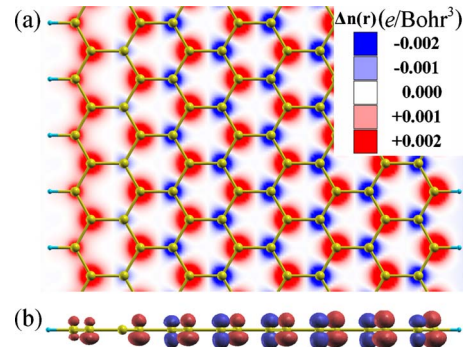


FIG. 3. (Color online) Spin densities of the monolayer ZGNR on Ni(111). (a) The spatial distribution of spin density on the xy plane. The difference between the spin densities of the majority (up) and minority (down) components is presented. (b) The side view of the spin density. The red and blue denote the up-spin and down-spin states, respectively. The isovalues are 0.002 e/bohr^3 .

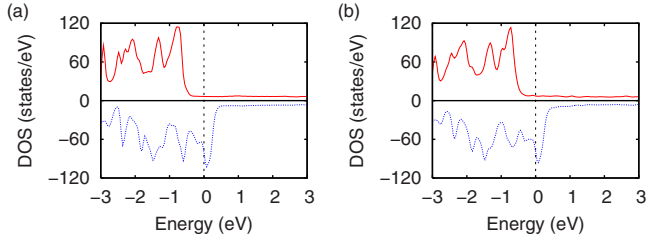


FIG. 4. (Color online) DOS of Ni atom. (a) DOS of the isolated Ni substrate and (b) PDOS of the Ni substrate in the ZGNR on Ni(111). The solid and dashed lines denote the up-spin and down-spin states, respectively. The energy is measured from the Fermi energy.

bitals and Ni d orbitals. The magnetic moments of the ZGNR on Ni(111) are not localized at the edges and are broadly distributed (Fig. 3). The atomic magnetic moment averaged over the C atoms in the ZGNR is less than $0.05 \mu_B/\text{atom}$ and is much smaller than those of freestanding ZGNRs having the APIES ($0.25 \mu_B/\text{atom}$) and PIES ($0.24 \mu_B/\text{atom}$) states at the edges. Therefore ZGNRs directly adsorbed on Ni(111) do not show flat-band magnetism. As is seen in Fig. 3, antiferromagnetic (AFM) coupling between the A and B sublattices is prominent. The projected DOS (PDOS) for all Ni atoms is similar to the DOS of the isolated Ni substrate (Fig. 4). The averaged atomic magnetic moment of the first Ni layer is $0.59 \mu_B/\text{atom}$ which is somewhat smaller than that of the isolated Ni substrate ($0.66 \mu_B/\text{atom}$).

B. Graphene on Ni

We next study the graphene on Ni(111). We use the unit cell which includes the two C and three Ni atoms. Whereas the isolated graphene has the nonmagnetic (NM) ground state, the graphene on Ni(111) has magnetic moments. Therefore, the PDOS for the graphene is drastically modified due to the effect of the FM Ni substrate (Fig. 5): whereas the DOS is zero at the Fermi level in the freestanding graphene [Fig. 5(a)], the DOS is not zero in the case of the graphene on Ni(111) [Fig. 5(b)]. We find AFM-like coupling between the A and B sublattices of the graphene, which is similar to that of the ZGNR on Ni(111) (Fig. 3). Since these two sublattices are nonequivalent because of the substrate, the magnetic moments are different: $0.021 \mu_B/\text{atom}$ and

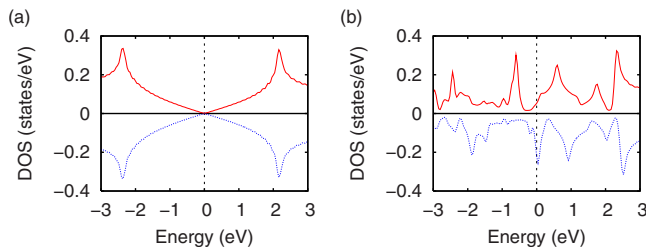


FIG. 5. (Color online) (a) DOS of the isolated graphene and (b) PDOS of the graphene in the graphene on Ni(111). Note that the isolated graphene is not AFM but NM. The solid and dashed lines denote the up-spin and down-spin states, respectively. The energy is measured from the Fermi energy.

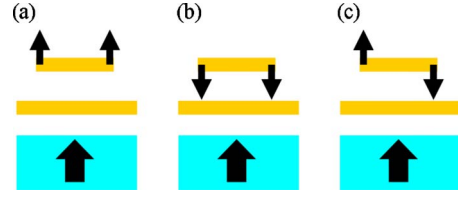


FIG. 6. (Color online) Magnetic structures of ZGNR/graphene on Ni(111). The PIES-1, PIES-2, and APIES states are shown in (a)–(c), respectively. The short and long slabs denote the ZGNR and graphene sheet, respectively. The rectangle denotes the Ni layer. The black arrows denote the direction of magnetic moments.

$0.027 \mu_B/\text{atom}$ for the up (majority)- and down (minority)-spin states, respectively.

C. ZGNR/graphene on Ni

Since it is expected that the graphene plays a role as a buffer layer on the Ni(111) substrate, we study the ZGNR/graphene on Ni(111) [Fig. 1(c)]. We consider the APIES state as well as PIES-1 (PIES-2) state where the spin direction of the ZGNR is the same as (different from) that of the Ni substrate (Fig. 6). We find that the PIES-1 state is the most stable: the difference between the total energies of the PIES-1 and APIES states is $4.2 \text{ meV}/\text{cell}$ and that between the total energies of the PIES-1 and PIES-2 states is $5.9 \text{ meV}/\text{cell}$. In the cases that the ribbon widths are 9 and 10, the PIES-1 state is also found to be the most stable. These results show that the magnetic interaction between the ZGNR edges and Ni substrate is *ferromagnetic*. Whereas the localized edge state disappears in the ZGNR on Ni(111), the ZGNR/graphene on Ni(111) has the localized edge state (Fig. 7). The magnetic moments at the two edges of the PIES-1 state ZGNR are $0.18 \mu_B/\text{atom}$ and $0.20 \mu_B/\text{atom}$ which are close to that of the freestanding ZGNR having the PIES state ($0.24 \mu_B/\text{atom}$).

The PDOS of the graphene sheet in the ZGNR/graphene on Ni(111) are very similar among the three magnetic states [Figs. 8(b), 8(d), and 8(f)] and are similar to the PDOS of the graphene sheet on Ni(111) [Fig. 5(b)]. Therefore, the PDOS of the graphene is affected very little by top layer ZGNRs. The PDOS of the ZGNR having the PIES-1 state shows that the two peaks near the Fermi level are broadened whereas those of the freestanding ZGNR having the PIES state are sharp [Figs. 2(a) and 8(a)]. On the other hand, the PDOS of the PIES-2 state is similar to that of the freestanding ZGNR

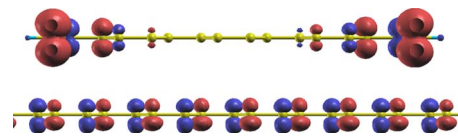


FIG. 7. (Color online) Isosurfaces of spin density of the PIES-1 state of ZGNR/graphene on Ni(111). The ZGNR plane (upper line) and graphene one (lower line) are presented and the Ni substrate is omitted. The red and blue isosurfaces denote the up-spin and down-spin states, respectively. These isovalues are $0.002 e/\text{bohr}^3$.

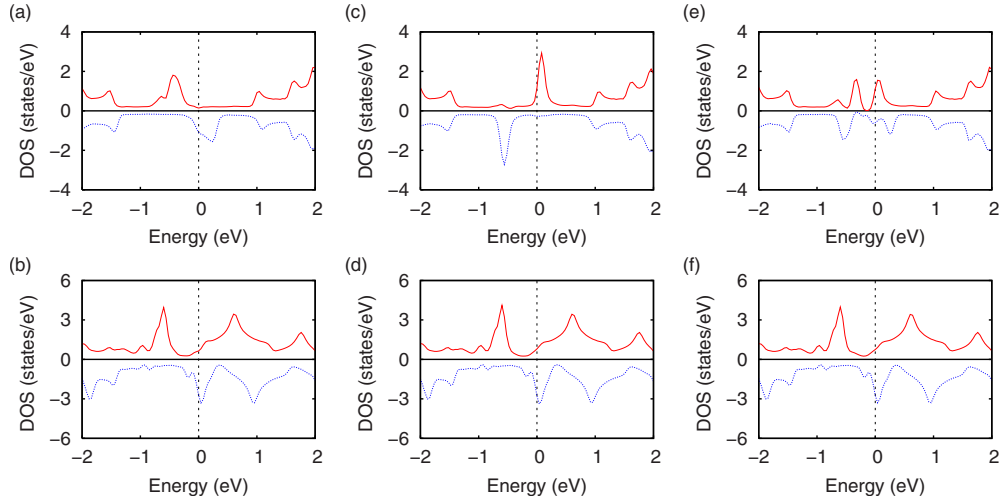


FIG. 8. (Color online) PDOS of the ZGNR and graphene sheet in ZGNR/graphene on Ni(111). The PDOS of the ZGNR for the PIES-1, PIES-2, and APIES states are shown in (a), (c), and (e), respectively, and that of the graphene for the PIES-1, PIES-2, and APIES states are shown in (b), (d), and (f), respectively. The solid and dashed lines denote the up-spin and down-spin states, respectively. The energy is measured from the Fermi energy.

having the PIES state [Figs. 2(a), 2(f), 2(i), 2(g), and 8(c)].

Here we discuss the relation of the PDOS of ZGNRs and the magnetic stability. In the case of the PIES-1 state, the locations of the peaks of the up (majority) and down (minority) near the Fermi level of the ZGNR are similar to those of the graphene: the up and down peaks are placed below and above the Fermi level, respectively [Figs. 8(a) and 8(b)]. These similar locations of the up and down peaks are expected to enhance the hybridization between the orbitals of the ZGNR and graphene and induce broadening of the PDOS of the ZGNR. On the other hand, in the case of the PIES-2 state, the PDOS peaks of the up-spin and down-spin states of the ZGNR are located above and below the Fermi level. Thus, the locations are opposite to those of the graphene where the peaks of the up-spin and down-spin states are located below and above the Fermi level. These opposite locations reduce the orbital hybridization and cause the fact that the peaks are not so broadened. The strong orbital hybridization of the PIES-1 state is expected to cause the fact that the PIES-1 state has lower energy than the PIES-2 state.

The peaks of the APIES state are somewhat broadened compared with those of the freestanding ZGNR having the APIES state [Figs. 2(b) and 8(e)]. This broadening due to the orbital hybridization is expected to lower the total energy of the APIES state. Therefore, its energy is lower than that of the PIES-2 state, though it is higher than that of the PIES-1 state.

We have discussed the effect of the orbital hybridization. Beside the orbital hybridization effect, the charge transfer from the substrate into the ZGNR affects the magnetic stability as was shown in a previous study.⁷ We find that electrons are injected into the ZGNR in the case of the three magnetic states. The Fermi level shifts upward from the case of the freestanding ZGNRs [Figs. 2(a), 2(b), 8(a), 8(c), and 8(e)]. For all three magnetic states, by using a fuzzy cell

partitioning method,²⁶ the number of injected electrons are estimated to be 0.1 e /cell in the ZGNR and 1.5 e /cell in the graphene sheet. The electron transfer from the substrate into the ZGNRs is expected to affect the magnetic stability. It is noted that previous DFT study of the graphene on Ni(111) (Ref. 19) found the electron transfers from the Ni substrate to the graphene, which is consistent with our results.

IV. SUMMARY

We have performed first-principles DFT calculations to clarify the magnetism of the monolayer ZGNR on Ni(111) and ZGNR/graphene on Ni(111). We studied ZGNRs whose ribbon widths are 1.8–2.2 nm. We found that the magnetic moments at the edges are small in the monolayer ZGNR on Ni(111) and do not show flat-band magnetism. On the other hand, in ZGNR/graphene on Ni(111), we found that magnetic moments of the edges are substantial and are close to those of the freestanding ZGNRs. The flat-band magnetism is recovered by the buffer graphene sheet. The magnetic ground state is the PIES-1 type [Fig. 6(a)]. We reveal the orbital hybridization between the edge C atoms of the ZGNR and graphene and electron injection induced by the charge transfer from the Ni(111) substrate to ZGNR. These features are expected to have a significant effect on the energetics of the magnetic state.

It is well known that the APIES state is the ground state of the freestanding ZGNR. However, we found that the PIES-1 state has 4.2 meV/cell lower energy than the APIES state in the ZGNR/graphene on Ni(111). Therefore, this study demonstrated that substrates have significant effects on the magnetism of ZGNRs. This finding is important for device applications of ZGNRs.

ACKNOWLEDGMENTS

This work was partly supported by Grants-in-Aid for Scientific Research (Grants No. 21560030 and No. 22016003) from the JSPS and by the Next Generation Super Computing Project, Nanoscience Program, MEXT, Japan and the RISS

project in IT program of MEXT. One of the authors (K.S.) thanks the JSPS for the financial support (Grant No. 21-2252). The computations in this research have been performed using the AIST Super Cluster facility at Tsukuba, the supercomputers at the ISSP, University of Tokyo, the RCCS, Okazaki National Institute, and the IMR, Tohoku University.

-
- ¹M. Ohishi, M. Shiraishi, R. Nouchi, T. Nozaki, T. Shinjo, and Y. Suzuki, *Jpn. J. Appl. Phys., Part 2* **46**, L605 (2007).
- ²N. Tombros, C. Jozsa, M. Popinciuc, H. T. Jonkman, and B. J. van Wees, *Nature (London)* **448**, 571 (2007).
- ³M. Nishioka and A. M. Goldman, *Appl. Phys. Lett.* **90**, 252505 (2007).
- ⁴M. Fujita, K. Wakabayashi, K. Nakada, and K. Kusakabe, *J. Phys. Soc. Jpn.* **65**, 1920 (1996).
- ⁵K. Nakada, M. Fujita, G. Dresselhaus, and M. S. Dresselhaus, *Phys. Rev. B* **54**, 17954 (1996).
- ⁶S. Okada and A. Oshiyama, *Phys. Rev. Lett.* **87**, 146803 (2001).
- ⁷K. Sawada, F. Ishii, M. Saito, S. Okada, and T. Kawai, *Nano Lett.* **9**, 269 (2009), and references therein.
- ⁸K. Kusakabe and M. Maruyama, *Phys. Rev. B* **67**, 092406 (2003).
- ⁹B. Sahu, H. Min, A. H. MacDonald, and S. K. Banerjee, *Phys. Rev. B* **78**, 045404 (2008).
- ¹⁰B. Sahu, H. Min, and S. K. Banerjee, *Phys. Rev. B* **81**, 045414 (2010).
- ¹¹B. Sahu, H. Min, and S. K. Banerjee, *Phys. Rev. B* **82**, 115426 (2010).
- ¹²G. Bertoni, L. Calmels, A. Altibelli, and V. Serin, *Phys. Rev. B* **71**, 075402 (2005).
- ¹³D. Eom, D. Prezzi, K. T. Rim, H. Zhou, M. Lefenfeld, S. Xiao, C. Nuckolls, M. S. Hybertsen, T. F. Heinz, and G. W. Flynn, *Nano Lett.* **9**, 2844 (2009).
- ¹⁴P. Sutter, M. S. Hybertsen, J. T. Sadowski, and E. Sutter, *Nano Lett.* **9**, 2654 (2009).
- ¹⁵J. Coraux, A. T. NeDiaye, C. Busse, and T. Michely, *Nano Lett.* **8**, 565 (2008).
- ¹⁶F. Varchon, R. Feng, J. Hass, X. Li, B. N. Nguyen, C. Naud, P. Mallet, J.-Y. Veuillen, C. Berger, E. H. Conrad, and L. Magaud, *Phys. Rev. Lett.* **99**, 126805 (2007).
- ¹⁷M. Ishigami, J. H. Chen, W. G. Cullen, M. S. Fuhrer, and E. D. Williams, *Nano Lett.* **7**, 1643 (2007).
- ¹⁸Y. Gamo, A. Nagashima, M. Wakabayashi, M. Terai, and C. Oshima, *Surf. Sci.* **374**, 61 (1997).
- ¹⁹P. A. Khomyakov, G. Giovannetti, P. C. Rusu, G. Brocks, J. van den Brink, and P. J. Kelly, *Phys. Rev. B* **79**, 195425 (2009).
- ²⁰T. Ozaki, H. Kino, J. Yu, M. J. Han, N. Kobayashi, M. Ohfuti, F. Ishii, T. Ohwaki, H. Weng, M. Toyoda, and K. Terakura, <http://www.openmx-square.org/>
- ²¹J. P. Perdew, K. Burke, and M. Ernzerhof, *Phys. Rev. Lett.* **77**, 3865 (1996).
- ²²N. Troullier and J. L. Martins, *Phys. Rev. B* **43**, 1993 (1991).
- ²³T. Ozaki, *Phys. Rev. B* **67**, 155108 (2003).
- ²⁴T. Ozaki and H. Kino, *Phys. Rev. B* **69**, 195113 (2004).
- ²⁵S. G. Louie, S. Froyen, and M. L. Cohen, *Phys. Rev. B* **26**, 1738 (1982).
- ²⁶A. D. Becke and R. M. Dickson, *J. Chem. Phys.* **89**, 2993 (1988).